Vortex melting in polycrystalline YBa$_2$Cu$_3$O$_7$ from ^{17}O NMR

A. P. Reyes, X. P. Tang, H. N. Bachman, and W. P. Halperin

Northwestern University and Science and Technology Center for Superconductivity, Evanston, Illinois 60208

J. A. Martindale* and P. C. Hammel

Los Alamos National Laboratory, Los Alamos, New Mexico 87545

(Received 4 March 1997)

Line-shape analysis of ^{17}O NMR spectra is used to probe vortex melting and dynamics in aligned powders of YBa$_2$O$_3$O$_7$. Vortex transitions are identified by comparing their dynamics with the NMR time scale. Line-shape changes indicate a well-defined melting transition at a temperature, T_m. Below T_m there is a coexistence regime of solid and liquid vortices with a lower bound, T_g, which marks complete vortex freezing. [S0163-1829(97)50822-8]

In layered superconductors extreme physical properties such as large anisotropy, short coherence length, and high transition temperatures combine to enhance thermal fluctuations leading to an exotic liquid vortex state. Although the behavior of the vortex liquid and its dynamics[1] are not yet well understood, the most detailed information has been obtained for clean single crystals. It is a challenge to extend this work to study materials relevant to technological applications—those having significant density of pinning sites, samples that are dirty, or that have some degree of disorder. It is important to develop new experimental probes of flux dynamics that are suitable for the study of such disordered materials. In this paper we present ^{17}O NMR results which provide unique insights into vortex lattice melting in aligned YBa$_2$Cu$_3$O$_7$ (YBCO) polycrystalline powders.

At sufficiently low temperatures it is expected that the magnetic field in the mixed state of a superconductor is characterized by a static, triangular ordered arrangement of flux lines, known as the Abrikosov vortex lattice. For superconductors with high transition temperatures, T_c, this lattice "melts" at a temperature $T_m < T_c$ when the amplitude of vortex fluctuations u becomes comparable to the intervortex spacing a_0: $\langle u^2(T_m)\rangle^{1/2} \sim c_L a_0$, where c_L is the Lindemann parameter. In YBCO and Bi-Sr-Ca-Cu-O (BSCCO) compounds various experimental techniques have been employed to detect vortex melting over a range of applied fields,[2–10] including muon spin resonance (μSR) line shape measurements,[11,12] a technique similar to the NMR method discussed here. In clean untwinned single crystals the melting line in YBCO is of first order and exhibits a power-law behavior: $H_m \sim (T_c - T_m)^{3/2}$, with values of $c_L \sim 0.14$–0.17.

One important issue is whether melting persists in the limit of zero driving force. A second problem is to understand the effect of crystalline disorder on the melting process. Recent magnetization measurements have revealed an unambiguous thermodynamic signature coincident with discontinuous changes in resistance in high-quality single crystals.[13] NMR provides an independent test of vortex melting while maintaining thermodynamic equilibrium. As a microscopic technique it is directly sensitive to the field distribution from the vortices including information on the time scale and spatial extent of their fluctuations. Additionally,

the ^{17}O NMR method has the potential for application to all oxide superconductors even in the presence of disorder.

Vortex melting may be detected using NMR as follows. Fluctuating vortices produce local fields at the nuclear sites which vary with a characteristic time τ_c. The NMR spectrum, obtained from Fourier transformation of the spin echo, represents the time average of these fluctuating fields over a period τ_e for spin-echo formation, a time that is controlled but is typically ~ 200 μs. When $\tau_c \ll \tau_e$, as would be expected for a liquid, the NMR linewidth is reduced due to motional narrowing. If the fluctuations are slow, $\tau_c \gg \tau_e$, as would be expected for a solid, averaging does not occur, and the NMR line is broad, reflecting the distribution of fields in the vortex state. When vortex freezing occurs the correlation time changes markedly in a short interval of temperature and can be observed through the corresponding changes in NMR line shape. The peak intensity in the NMR spectrum in the normal and liquid state is determined by the average field B. This frequency shifts abruptly at $T = T_m$ when the vortices freeze. The frozen structure has a characteristic field distribution which peaks at the saddle point located midway between two vortices. The saddle-point field is lower than the average field B by a factor proportional to ϕ_0/λ^2, where ϕ_0 is the flux quantum ($=2.07 \times 10^{-7}$ G cm^2) and $\lambda(T)$ is the T-dependent London penetration depth.[14] The variance (second moment) of this distribution,[15]

$$\langle \Delta B^2 \rangle \approx 0.0037 (\phi_0/\lambda^2)^2 \tag{1}$$

is independent of field for $H_{c1} \ll B \ll H_{c2}$. Vortex melting is observable by NMR if the normal-state linewidth $1/T_2^*$ $\ll \gamma \langle \Delta B \rangle^{1/2}$, where γ is the nuclear gyromagnetic ratio. In YBCO for $H \| c$, $\lambda = \lambda_{ab}(0) \sim 1400$ Å and $\langle \Delta B^2 \rangle^{1/2}(T=0) \sim 65$ G. The ^{17}O nucleus ($\gamma = 0.5772$ MHz/kOe) satisfies this criterion, with linewidth of ~ 7 G at T_c. In comparison, ^{63}Cu has ~ 60 G and ^{89}Y has ~ 5 G. Earlier work with ^{89}Y NMR provided the first NMR evidence of the effect of vortex motion on spectral linewidths.[16] In general ^{89}Y NMR measurements are hindered by long spin-lattice relaxation times, T_1, which reduce signal to noise and limit study at low magnetic fields.
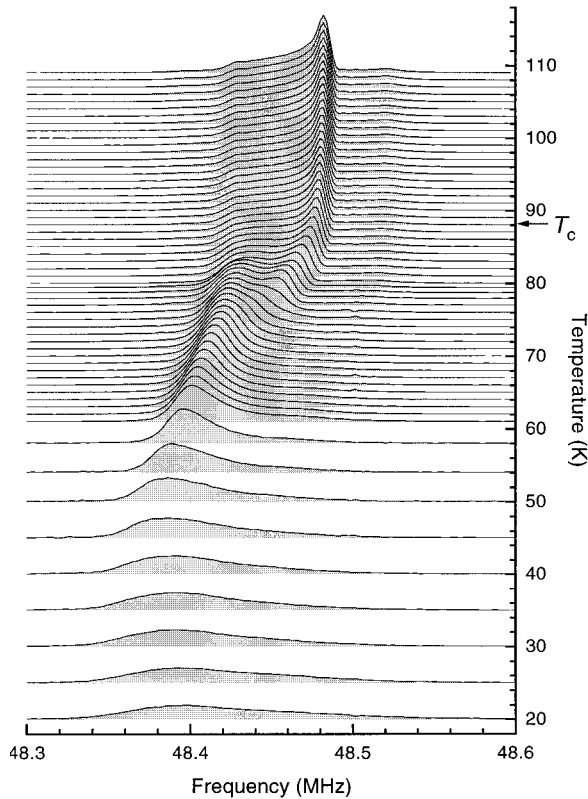
<u>55</u>   R14 737

FIG. 1. Temperature dependence of the O(2,3) central transition at 8.4 T for which T_c is shown. Each spectrum is normalized to unity.
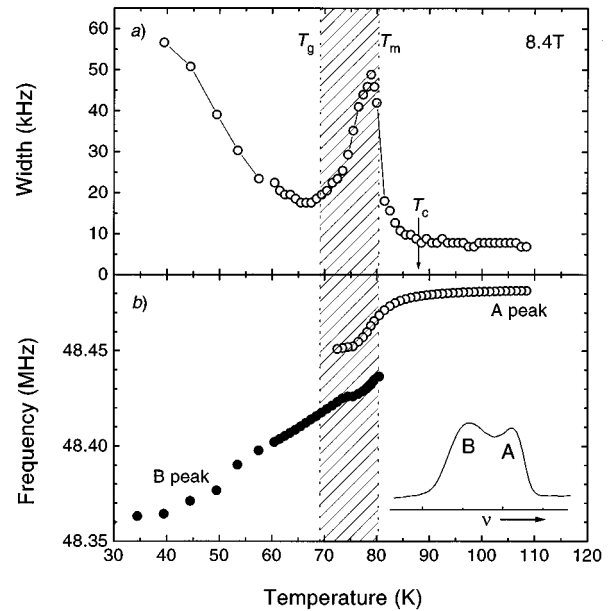

FIG. 2. (a) Temperature dependence of NMR linewidth at 8.4 T. The shaded area defines the coexistence region for liquid and solid vortices. (b) Temperature dependence of resonance frequencies of the A (open circles) and B (closed circles) peaks. Inset: Spectrum at 78 K.

Powder specimens of 30–40 % ^{17}O-enriched YBa$_2$Cu$_3$O$_{6.95}$ were prepared by solid-state reaction and magnetically aligned, as described in Ref. 17. Low-field magnetization data shows a sharp T_c at 92.5 K. The spectra were obtained by Fourier transforming the spin echo in a fixed magnetic field. Short (<2 μs) tipping pulses and the standard $\pi/2-\tau-\pi$ pulse sequences ($\tau\sim150$–200 μs) were used producing an echo at $\tau_e=2\tau$. The central $\langle-\frac{1}{2}\leftrightarrow\frac{1}{2}\rangle$ transition of the planar oxygens O(2,3) was obtained with repetition times ~14–20 ms that eliminated signals from the apical sites O(4) which have a T_1 100 times longer. The temperature stability was ±0.1 K. No hysteresis was observed in comparing field-cooled and zero-field cooled spectra or spectra obtained by cooling and warming.

A typical temperature dependence at 8.4 T of the central transition spectrum of the planar O(2,3) is shown in Fig. 1. The characteristic normal-state line shape has a low frequency tail,^{18} likely due to slight oxygen deficiency. As the sample is cooled, the shape of the spectrum evolves from a narrow unshifted line to an anomalous double-peak structure appearing at a temperature, T_m. This structure is maintained down to a temperature at which the higher frequency peak disappears. Below this temperature, which we label T_g, there is a single broad peak at a lower frequency. We observe these features at all magnetic fields. In Fig. 2(a) we quantitatively characterize these line-shape features in a model independent way by plotting the full width at $\frac{2}{3}$ maximum height. From this plot we see that the narrow normal-state linewidth persists below T_c until a sharp increase occurs at the onset of the double-peak structure described above. At

lower temperatures the decrease in the linewidth marks the disappearance of this structure. Thus, the peak in Fig. 2(a) serves *unambiguously* to define the temperatures T_m and T_g.

To better understand the temperature dependence of the spectra we performed nonlinear least-squares analysis of the composite line shapes. We modeled the spectra to consist of a normal-state line shape part ''A'' and a Gaussian part ''B.'' In Fig. 2(b) we plot the resulting peak frequencies of these two components. The A component shows a small frequency shift relative to its normal-state position just below T_c, attributable to the usual reduction of Knight shift due to electron pairing in the superconducting state. At T_m the B component appears, consistent with the sharp increase in linewidth in Fig. 2(a). At T_g the A component disappears, also consistent with Fig. 2(a). We emphasize that the observation of two components demonstrates the simultaneous existence of two distinct regions of the sample associated with spectral components A and B. Our line-shape analysis shows that as the temperature is decreased, the A component intensity decreases continuously from 100% to zero as the B component intensity increases correspondingly.

We interpret these observations in terms of vortex dynamics. The A component represents a motionally narrowed NMR spectrum expected from a vortex liquid below T_c; and the B component characterizes the field distribution in the solid lattice below T_g, with a large saddle-point shift. In the coexistence region, $T_g<T<T_m$, there are both liquid and solid regions present in the sample at the same time. At temperatures below T_g, the linewidth steadily increases, as is expected for a rigid vortex lattice in which the penetration depth decreases with decreasing temperature. The observed effects are not due to a distribution in T_c's in the sample
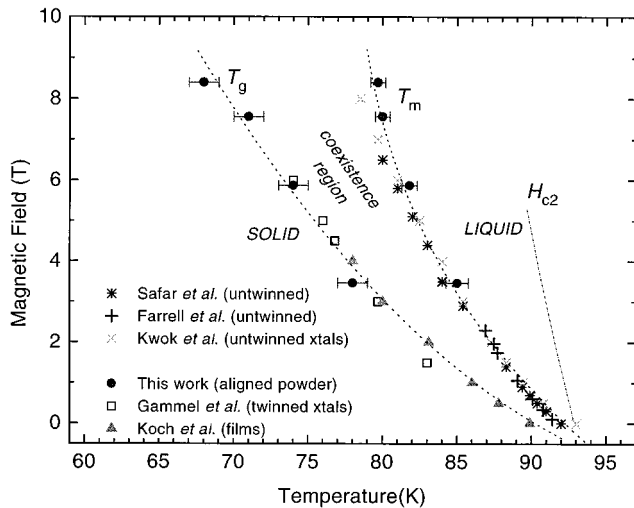
FIG. 3. H-T phase diagram for different YBCO samples. The error bars depict finite temperature steps in the NMR spectra. T_m and T_g are obtained from Fig. 2 as described in the text. No correction has been applied for differences in $T_c(0)$ for different samples (Refs. 3, 4, 7, 8, and 22). The H_{c2} line is from Ref. 20. Lines through T_m and T_g are guides to the eye.

since there is no evidence for this in the low-field magnetization. Furthermore, the whole spectrum exhibits Knight-shift reduction due to superconductivity at $T_c(H)$. We have observed a similar effect in ^{205}Tl NMR in Tl$_2$Ba$_2$CuO$_6$ but the double-peak structure is not as well defined.[19] The ^{89}Y NMR in YBCO has not resolved these effects.[16]

The temperatures T_g and T_m at different fields are plotted in a H-T melting phase diagram shown in Fig. 3, together with results obtained from other experiments. The behavior for clean untwinned YBCO crystals is very well established while the melting transition in "dirty" samples with disorder, twins, and grain boundaries, is more ambiguous and less well characterized. The transitions in the latter case follow the irreversibility line and are explained in terms of thermally activated depinning.[21] As shown in Fig. 3, twinned single crystals and films have consistently lower transitions. Kwok et al.[22] systematically studied the effects of disorder and, for example, observed that melting in twinned crystals occurs only in an off-c axis field geometry because the vortices are confined by twin boundaries. They found that the first-order transition is suppressed and the transition is broader and smoother. Similarly, in radiation damaged crystals the high density of defects suppresses the transition that appears second-order-like at lower temperatures. In contrast, our NMR results show an unambiguous melting transition in a powder sample, which can be thought of as "dirty." The agreement of our T_m values with those for untwinned crystals suggests that they are of common origin and are likely intrinsic to the material. Our slightly higher temperatures for T_m might indicate that we observe the onset of twin boundary pinning just above T_m as discussed by Fleshler et al.[22] We note that Worthington et al.[23] observed two transitions in defect-enhanced crystals below T_c—the first being a remnant of first-order melting of the clean crystal at T_m and another, of second order, at a lower temperature which is consistent with our observation of T_g. They attributed the lower tem-
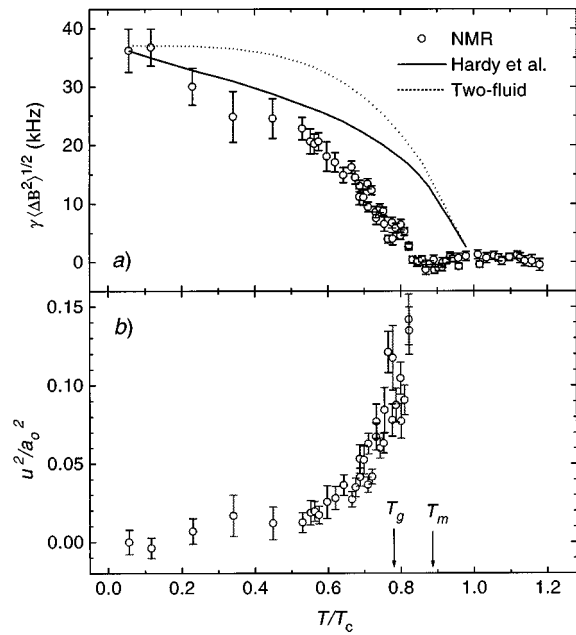

FIG. 4. (a) Second moment as a function of temperature at 8.4 T. The normal-state contribution has been subtracted from the data. The solid line is derived from Ref. 24. The dotted line is calculated from the two-fluid model. The temperature at which the second moment increases is consistent with our identification of T_m. (b) Temperature dependence of the mean-square displacement ratio.

perature anomaly to a vortex-glass transition. The observations are similar to our NMR results.

The spectrum shape for rigid vortices at temperatures $T < T_g$ can be expected to be consistent with Eq. (1). However, we find the temperature dependence of the second moment, $\gamma \langle \Delta B^2 \rangle^{1/2} = \sigma$, to be always less than that for rigid vortices as shown in Fig. 4(a). For comparison we show the rigid lattice second moment calculated from Eq. (1) with $\lambda_{ab}(T)$ using the two-fluid model and the microwave data of Hardy et al., taking $\lambda_{ab}(0) = 1400$ Å.[24,1] The NMR σ remains constant at the normal-state value and steadily increases below T_m approaching the rigid lattice value at low temperatures. Similar observations have been made using μSR on BSCCO.[12] This behavior could be interpreted as due to either fast thermal fluctuations of vortices or to vortex diffusion.[14,16,25] Both mechanisms invoke motional narrowing which requires fluctuations much faster than $1/\tau_e$. However, from our measurements of spin-spin relaxation rates, found by varying τ_e, we know that the vortex fluctuation time $\tau_c \gg \tau_e$ for $T < T_g$.[26] Consequently, we offer an alternate explanation, one first suggested by Brandt[15] and which was later invoked by S. L. Lee et al.[12] to understand μSR line-shape reduction in BSCCO.

Perturbation of stiff flux lines generally increases the field variance. However, Brandt[15] argued that in a layered system small transverse displacement of various segments of a flexible flux line lead to a decrease of the field distribution owing to partial destructive interference from the different segments, thus modifying the NMR line shape. In order to observe NMR line narrowing, the displacements need not occur in adjacent layers. Rather, it is sufficient that they show spatial variations on a distance scale less than that over which the fields are averaged, namely the penetration depth,

$\lambda_{ab}(T)$, which diverges as T_c is approached. Furthermore, the time scale for fluctuations must be slower than τ_e. This is reasonable for a weakly anisotropic system such as YBCO. Brandt showed that the field variance is given by

$$\sigma^2/\sigma_0^2 \sim [\exp(-26.3u^2/a_0^2) + 24.8u_l^2/a_0^2 \ln \kappa] \qquad (2)$$

where σ_0 is the perfect (rigid) lattice width, $\mu^2 = u_p^2 + u_l^2$ and u_p, u_l are vortex segment and vortex line displacements about equilibrium positions. For the solid state at low temperatures, $u^2/a_0^2 \ll 1$. Our observation that $\sigma < \sigma_0$ suggests that the first term dominates Eq. (2) and so we neglect the second term. As mentioned above, this approximation becomes progressively better at higher temperatures. Consequently, the temperature dependence of $(u^2/a_0^2)^{1/2}$ can be obtained directly from the linewidth data. These ratios are shown in Fig. 4(b) and appear to be linear at low temperatures. At the temperature T_g, $(u^2/a_0^2)^{1/2} \sim 0.28$. This ratio is a measure of the static disorder from the straight line perfect vortex lattice. Interestingly, it is of similar magnitude as the Lindemann parameter based purely on thermal displacements obtained from other experiments[5,6] (~ 0.2) and from that calculated using the continuum elastic theory (~ 0.4) found from fitting the T_g line of Gammel *et al.*[8,27]

On this basis it seems reasonable that the vortices have significant transverse displacements deviating from straight lines at low temperatures caused by random pinning along their lengths. In this regime we see an inhomogeneously broadened NMR spectrum characteristic of an inhomogeneous solid vortex structure with $\tau_c \gg \tau_e$. As the temperature is increased the penetration depth increases, more effectively averaging the local fields. At sufficiently high temperatures thermal activation allows some segments of the flux lines to overcome pinning and to have sufficient amplitude to melt, consistent with the Lindemann criterion. This process starts at $T \sim T_g$. Coexistence of pinned and unpinned vortex segments is evident in the temperature region $T_g < T < T_m$ where we observe a composite NMR line shape. As fluctuations increase the liquidlike peak becomes narrower and more enhanced since more vortex segments are depinned and contribute more to the spectral weight. When $T = T_m$ the vortices are totally unpinned leaving a vortex liquid indicated by a single narrow (*A* peak) spectrum. The transition temperature T_m should be intrinsic to the material. However, the width of the coexistence region is likely to be sample dependent and wider for samples with greater density of pinning sites, as may be the case with thin films. Clean and untwinned crystals may not exhibit such coexistence at all.

In summary, we have used ^{17}O NMR to prove the vortex field-temperature phase diagram in $YBa_2Cu_3O_7$ and find for aligned polycrystalline samples that there is a coexistence of liquid and solid vortex behavior in a range of temperatures at fixed field. We interpret the NMR spectra in terms of thermal depinning of flexible flux lines in a weakly anisotropic system.

---

*Present address: Department of Physics, The Ohio State University, Columbus, Ohio 43210.

[1] For reviews see G, Blatter *et al.*, Rev. Mod. Phys. **66**, 1125 (1994); D. J. Bishop *et al.*, Science **255**, 165 (1992).

[2] P. L. Gammel *et al.*, Phys. Rev. Lett. **61**, 1666 (1988).

[3] D. E. Farrell *et al.*, Phys. Rev. Lett. **67**, 1165 (1991).

[4] R. H. Koch *et al.*, Phys. Rev. Lett. **63**, 1511 (1989).

[5] M. Charalambous *et al.*, Phys. Rev. B **45**, 5091 (1992).

[6] W. K. Kwok *et al.*, Phys. Rev. Lett. **69**, 3370 (1992); **72**, 1092 (1994).

[7] H. Safar *et al.*, Phys. Rev. Lett. **69**, 824 (1992).

[8] P. L. Gammel *et al.*, Phys. Rev. Lett. **66**, 953 (1991).

[9] C. D. Keener *et al.*, Phys. Rev. Lett. **78**, 1118 (1997).

[10] E. Zeldov *et al.*, Nature (London) **375**, 373 (1995).

[11] J. E. Sonier *et al.*, Phys. Rev. Lett. **72**, 744 (1994).

[12] S. L. Lee *et al.*, Phys. Rev. Lett. **75**, 922 (1995).

[13] U. Welp *et al.*, Phys. Rev. Lett. **76**, 4809 (1996).

[14] Y. Q. Song *et al.*, Phys. Rev. Lett. **70**, 3127 (1993).

[15] E. H. Brandt, Phys. Rev. Lett. **66**, 3213 (1991).

[16] P. Carretta and M. Corti, Phys. Rev. Lett. **68**, 1236 (1992); B. J. Suh *et al.*, *ibid.* **71**, 3011 (1993); H. B. Brom and H. Alloul, Physica C **177**, 297 (1991).

[17] M. Takigawa *et al.*, Phys. Rev. Lett. **63**, 1865 (1989).

[18] The tail is not due to misalignment since there are no powder patterns at these spectral positions.

[19] X. P. Tang, Ph.D. thesis, Northwestern University, 1996.

[20] U. Welp *et al.*, Phys. Rev. Lett. **62**, 1908 (1989).

[21] Y. Xu *et al.*, Phys. Rev. B **43**, 5516 (1991); L. Civale *et al.*, *ibid.* **43**, 5425 (1991).

[22] W. K. Kwok *et al.*, Physica B **197**, 579 (1994); S. Fleshler *et al.*, Phys. Rev. B **47**, 14 438 (1993).

[23] T. K. Worthington *et al.*, Phys. Rev. B **46**, 11 854 (1992).

[24] W. N. Hardy *et al.*, Physica B **197**, 609 (1994).

[25] L. I. Glazman and A. E. Koshelev, Phys. Rev. B **43**, 2835 (1991).

[26] A. P. Reyes *et al.* (unpublished).

[27] A. Houghton *et al.*, Phys. Rev. B **40**, 6763 (1989).